Popular Summary

Validation and Determination of Ice Water Content – Radar Reflectivity Relationships during CRYSTAL-FACE: Flight Requirements for Future

D. S. Sayres[1], J.B. Smith[1], J.V. Pittman[1,5], E.M. Weinstock[1], J.G. Anderson[1], G. Heymsfield[2], L. Li[3], A.M. Fridland[4], A.S. Ackerman[4]

[1]Department of Earth and Planetary Sciences, Harvard University
[2]Goddard Space Flight Center
[3]UMBC/GEST
[4]NASA Goddard Institute for Space Studies
[5]Marshall Space Flight Center

In order for clouds to be more accurately represented in global circulation models (GCM), there is need for improved understanding of the properties of ice such as the total water in ice clouds, called ice water content (IWC), ice particle sizes and their shapes. Improved representation of clouds in models will enable GCMs to better predict for example, how changes in emissions of pollutants affect cloud formation and evolution, upper tropospheric water vapor, and the radiative budget of the atmosphere that is crucial for climate change studies. An extensive cloud measurement campaign called CRYSTAL-FACE was conducted during Summer 2002 using instrumented aircraft and a variety of instruments to measure properties of ice clouds. This paper deals with the measurement of IWC using the Harvard water vapor and total water instruments on the NASA WB-57 high-altitude aircraft. The IWC is measured directly by these instruments at the altitude of the WB-57, and it is compared with remote measurements from the Goddard Cloud Radar System (CRS) on the NASA ER-2. CRS measures vertical profiles of radar reflectivity from which IWC can be estimated at the WB-57 altitude. The IWC measurements obtained from the Harvard instruments and CRS were found to be within 20-30% of each other. Part of this difference was attributed to errors associated with comparing two measurements that are not collocated in time an space since both aircraft were not in identical locations. This study provides some credibility to the Harvard and CRS-derived IWC measurements that are in general difficult to validate except through consistency checks using different measurement approaches.

Validation and determination of ice water content - radar reflectivity relationships during CRYSTAL-FACE: Flight requirements for future comparisons

D. S. Sayres,[1] J. B. Smith,[1] J. V. Pittman,[1,5] E. M. Weinstock,[1] J. G. Anderson,[1] G. Heymsfield,[2] L. Li[3] A. M. Fridlind[4] A. S. Ackerman[4]

D. S. Sayres, Department of Earth and Planetary Sciences, Anderson Group/CCB, Harvard University, 12 Oxford Street, Link 261, Cambridge, MA 02138. (sayres@huarp.harvard.edu)

[1]Department of Earth and Planetary Sciences, Harvard University, Cambridge, MA 02138

[2]Goddard Space Flight Center, NASA, Greenbelt, MD 20771

[3]University of Maryland, Baltimore County, Baltimore, MD 21250

[4]NASA Goddard Institute for Space Studies, New York, NY 10025

[5]Marshall Space Flight Center, NASA, Huntsville, AL 35805

Abstract. In situ measurements of cirrus ice water content (IWC) by the Harvard waper vapor and total water instruments onboard the NASA WB-57 during CRYSTAL-FACE are compared with remote sensing data made by the Cloud Radar System (CRS) instrument from the NASA ER-2. The comparisons are used to show that for measurements of in situ IWC and remotely measured radar reflectivity (Z_e) collocated within 2 kilometers of each other, a single IWC-Z_e relationship can be found that fits the data with an uncertainty of $\pm$20-30%. A cloud resolving model shows this level of uncertainty to be consistent with sampling errors associated with comparing two measurements that are not collocated. Satellite-borne remote sensing measurements from CloudSAT and CALIPSO will soon provide the vertical structure of clouds on a global scale. Uncertainties are quantified in the use of in situ data to validate the retrieval algorithms used to derive the IWC of clouds from remote sensing observations, such as radar reflectivity (Z_e). Uncertainties are classified into instrumental uncertainties, uncertainties related to sampling errors, and uncertainties in using a single IWC-Z_e relationship to describe a cloud.

1. Introduction

Clouds play a critical role in determining the radiative budget of the atmosphere and surface by the absorption and scattering of solar and terrestrial radiation [*Norris*, 2000]. The extent to which clouds scatter and absorb radiation is determined by the microphysical and geometric structure of the cloud [*Baran*, 2005]. In order for clouds to be represented more accurately in GCMs the vertical structure of ice water content (IWC), particle size distribution, and particle geometry (habit) in clouds needs to be obtained on a global scale [*Stephens et al.*, 2002]. Accurately representing clouds in general circulation models (GCMs) and climate models is paramount for enabling models to predict how changes in emissions of pollutants will affect cloud formation and evolution, upper tropospheric water vapor, and the radiative budget of the atmosphere. However, to date cloud processes represent one of the largest uncertainties in GCMs [*Stephens*, 2005].

In order to improve our understanding of cloud physics several measurement campaigns using balloon and aircraft *in situ* measurements have been devoted to studying the micro and macrophysical properties of clouds [*Pawlowska et al.*, 2000; *Gultepe et al.*, 2001; *Buschmann et al.*, 2002; *Nasiri et al.*, 2002, and references therein]. While *in situ* measurements provide high spatial resolution, they typically provide only a one dimensional trajectory through a cloud and within the limit of aircraft flight time can only sample a small fraction of a cloud. In recent years remote sensing probes such as radar and lidar have become central to the effort to quantitatively measure microphysical properties of clouds on a large scale. The culmination of this effort is NASA's launch of a suite of satellites known as the A-Train [*Stephens et al.*, 2002]. The A-Train consists of six satellites

flying in formation so that all make observations of the same volume of atmosphere within 15 minutes of each other. CloudSat, a 94 GHz cloud profiling radar, and CALIPSO, a two channel (532 and 1064 nm) cloud and aerosol lidar, are focused on making high resolution measurements of the microphysical properties of clouds such as IWC, median ice particle volume diameter, and particle shape.

The physical properties of clouds are deduced by remote sensing instruments from the attenuation and scattering of radar and lidar signals or by their infrared emission. Radar instruments measure the reflectivity from cloud particles caused by the angular dependence of scattering of the radar beam. The reflectivity, Z_e, can be related related to the IWC of the cloud via a power-law relationship detailed in section 2. Since different clouds, and regions within a cloud, possess different particle-size distributions, habits, and ice densities, a suite of relationships, each set representing a particular category of cloud, is required to describe an ensemble of cloud types. To determine which relationship to use for a particular cloud and to minimize the uncertainty in the IWC-Z_e relationships, several approaches have been suggested using the extinction coefficient from lidar [*Wang and Sassen*, 2002a, b], the mean Doppler velocity [*Donovan*, 2003], or cloud top temperature [*Liu and Illingworth*, 2000]. However, given the ability to categorize clouds based on remote measurements, great importance still must be placed on obtaining and validating coefficients for each cloud type.

The first step in deriving IWC-Z_e relationships for different clouds is to obtain IWC and the corresponding Z_e. Previous comparisons have used *in situ* particle size data [*Brown and Illingworth*, 1995; *Liu and Illingworth*, 2000] or modeled size spectra of pure hexagonal columns and plates to derive IWC and Z_e [*Aydin and Tang*, 1997; *Sassen et al.*,

2002]. These studies have reported uncertainties in the derived IWC of as much as 60% for a given value of Z_e. For the comparison presented here we use direct measurements of *in situ* IWC and remotely detected radar reflectivity obtained during the Cirrus Regional Study of Tropical Anvils and Cirrus Layers - Florida Area Cirrus Experiment (CRYSTAL-FACE) [*Jensen et al.*, 2004].

The interpretation of this comparison is complicated by the spatial and temporal differences between the air parcels that the *in situ* and remote instruments measure. To address the uncertainties inherent in comparing IWC from *in situ* and remote measurements we group the uncertainties into three categories, not only to best constrain the parameters that are needed to derive IWC from Z_e, but also to try to determine the most efficient way to carry out these validation experiments.

1. Instrumental uncertainties in the measurement of IWC and radar reflectivity. These uncertainties are assumed to be fixed for a given comparison and independent of the cloud being measured.

2. Uncertainty in matching *in situ* data with remote data, which we refer to as sampling error. This error occurs due to the reality that there is often spatial or temporal separation between the *in situ* measurement and the remote measurement. Due to the large variability of IWC, or cloud inhomogeneities, measurements that are not collocated can lead to erroneous (non-instrumental) errors in the comparison.

3. Uncertainty in the relationships used to calculate IWC from Z_e. This uncertainty includes the sensitivity of the constants used in this calculation to variations in habit, size distribution, and ice density. This category also includes estimates of the uncertainty resulting from cloud type variability.

Instrumental uncertainties and the error in derived IWC are discussed in Section 3.1. Section 3.2 discusses the comparisons made during the CRYSTAL-FACE mission and the uncertainty associated with using different IWC-Z_e relationships. Section 4 uses a cloud model to evaluate the error associated with insufficient overlap between two instrument measurements.

2. Physical basis for the IWC-Z_e relationship

The magnitude of the radar reflectivity, Z, due to Rayleigh scattering is proportional to $\int n(D)D^6\,dD$, where n is the number density of particles with diameter, D [*Liao and Sassen*, 1994]. However, this is only valid for small spheroidal particles and does not account for Mie scattering or the effect of particle shape and density. Equation 1 is a modified form of this relationship proposed by *Liu and Illingworth* [2000], where a term accounting for particle shape has been added.

$$Z = \int n(D)D^6K(m,\rho)^2 f(D,\rho)h(D,\rho)/0.93\,dD, \tag{1}$$

where K is a factor dependent on the refractive index of ice, m, f is the ratio of Mie to Rayleigh scattering, h is a shape factor dependent upon the habit of the particles, and the factor 0.93 is chosen so that for liquid water the relationship reduces to the equation for spheroidal droplets.

IWC, defined as the mass of ice per unit volume of air, can be written as

$$IWC = \int \rho V n(D)\,dD, \tag{2}$$

where n is the number density of particles with volume, V, and mass density, ρ. By inspection of Equations 1 and 2, Z is proportional to the square of IWC. The relationship between IWC and Z_e, the equivalent reflectivity for ice, can thus be written as a power

law,

$$IWC = aZ_e^b, \tag{3}$$

where IWC is measured in g/m^3, Z_e is measured in mm^6m^{-3}, and a and b are functions of particle size distribution, habit, and ice density. Given measurements of IWC and corresponding Z_e values, the coefficients a and b are determined empirically by regression of IWC with Z_e.

3. Direct comparisons of *in situ* IWC and remote Z_e data

The CRYSTAL-FACE campaign took place out of Key West, Florida during July, 2002. The main focus of the mission was to study the physical properties of subtropical cirrus clouds in order to improve our understanding of the formation and evolution of cirrus and to improve our ability to model cirrus in GCMs. In order to accomplish this objective, several aircraft were used, each carrying a different suite of instruments and each measuring a different level of the atmosphere. Another goal of CRYSTAL-FACE was to compare and validate remote sensing instruments flown on the ER-2 with *in situ* measurements from the WB-57. The ER-2 carried remote sensing instruments similar to those that are part of the A-Train constellation of satellites. The Cloud Radar System (CRS) and Cloud Physics Lidar (CPL) have similar capabilities to the instruments aboard the CloudSat and CALIPSO Satellites, respectively. The WB-57 carried a suite of *in situ* instruments measuring IWC (Harvard Total Water and Water Vapor), particle size distributions, habit, and aerosols, as well as tracer and meteorological measurements.

3.1. Flight Plans and Instruments

As an example of coordinated flight segments used to compare remote and in situ IWC measurements, we show in figure 1 the flight track of the WB-57 (left image) and ER-2 (right image) during the flight of July 16th. The ER-2 made several passes over a convective system that developed over Florida and moved westward, while the WB-57 made several passes through the cirrus outflow of the same convective system. This makes the flight of July 16th ideal for comparing remote and *in situ* data. While during other flights the ER-2 and WB-57 flew together, they were sampling several different clouds and therefore did not sample air parcels close enough in time and space to make reasonable comparisons. For the purpose of this comparison we focus on IWC retrieved from radar and measured *in situ*. Radar reflectivity was measured using the Cloud Radar System (CRS) instrument that flew aboard the ER-2 aircraft and IWC was measured using the Harvard Lyman-α total water (HV-TW) and water vapor hygrometers aboard the WB-57.

The CRS instrument is a 94 GHz Doppler, polarimetric radar mounted in the right wing pod of the ER-2 [*Li et al.*, 2004]. The 94 GHz frequency allows CRS to measure a wide range of clouds, from thin cirrus to thick convective anvils. The units of reflectivity (Z_e) are mm^6m^{-3}. However, Z_e is often reported in units of power (dB) where $1\,dB = 10log_{10}(mm^6m^{-3})$. The sensitivity of the CRS instrument is -29 dB ($3.65 \times 10^{-3}g/m^3$ of condensate) allowing it to detect 99% of radiatively significant clouds at midlatitudes and 92% in the tropics [*Brown and Illingworth*, 1995]. Radiatively significant clouds are defined as those that cause differences from clear sky values of more than 10 Wm^{-2} in outgoing longwave radiation or in the longwave flux divergence within a cloud layer and 5 Wm^{-2} in the downward longwave flux. To maintain the calibration of the radar, average transmit power and receiver gain are continuously monitored in order to have in-flight

diagnostics as to the transmitter stability. In addition, external calibration against other radar systems yields an uncertainty of 1 dB, which is equivalent to a 15% uncertainty in the retrieved IWC. The spatial resolution of the reflectivity data reported by the CRS instrument for the CRYSTAL-FACE mission is 1 km horizontally and 75 meters vertically along the flight path of the ER-2 . A retrieval algorithm using the *Brown and Illingworth* [1995] relationship was used to calculate the archived remote IWC data. The coefficients used for the retrieval are derived from ice crystal size spectra from a 2D optical array probe sampling cirrus from midlatitude frontal systems. The size spectra are converted to IWC and radar reflectivities via equations similar to Equations 2 and 1, respectively. For the IWC the bulk density is assumed to be proportional to $D^{-1.1}$, where D is the mean volume diameter of the particles. A simple least squares fit to Equation 3 yields the parameters a and b. The CRS data use a K^2 value of 0.695 which is appropriate at 94 GHz under 0°C conditions. However, previous measurements have used K^2 equal to 0.93 in order that the reflectivities be scaled to liquid water. In order to compare the data presented here with previous measurements, we have rescaled the CRS data by subtracting 1.26 dB.

HV-TW measures total water (i.e. vapor + ice) directly. IWC is derived by subtracting water vapor, as measured by the Harvard water vapor instrument, from total water. Both Harvard water vapor and total water measure water vapor by using Lyman-α to photodissociate water into an OH fragment in its first excited electronic state. The excited OH fragment then either relaxes via fluorescence or is quenched during a collision with an air molecule. Within the range of ambient densities encountered during CRYSTAL-FACE,

the magnitude of the fluorescence signal is directly proportional to the mixing ratio of water.

Calibrations are performed at a range of pressures and water vapor mixing ratios [*Weinstock et al.*, 2006a]. Water vapor is injected into the calibration system using a bubbler and checked via longpath and shortpath (axial) absorption. The calibration is therefore tied to two fundamental standards: the vapor pressure of water over liquid at room temperature and the absorption cross section of water vapor at the Lyman-α wavelength. In-flight validation consists of cross checking changes in the ambient water vaper mixing ratio (i.e. ΔH_2O) using both dual-path (axial) absorption and fluorescence. In addition, in clear air, the Total Water instrument is compared to the Water Vapor instrument. Agreement between the two instruments increases confidence in the water vapor measurement and the IWC product [*Weinstock et al.*, 2006b].

During flight operation, the HV-TW instrument uses a roots pump downstream of the detection axis to pull ice particles and water vapor into the instrument duct while maintaining isokinetic flow to ensure that the number density of particles entering the inlet is the same as the ambient number density. A 600-Watt inlet heater evaporates the ice particles and the total water is measured. The precision of the total water instrument is 5% and the accuracy with respect to ice water content is 15% [*Weinstock et al.*, 2006a]. The HV-TW uses a 1 second integration time and due to the speed of the aircraft this yields a horizontal resolution of 100-200 meters. For the purposes of this comparison, 10 second data, which produces 1.5 km averages, are used in order to make the horizontal resolution consistent with that of the CRS instrument.

3.2. Direct Comparison of Data

If both the ER-2 and WB-57 were coordinated so that the instruments were always sampling the same footprint at the same time, then a direct comparison between the instruments would be straightforward. However, because of constraints on aircraft velocities and air traffic control, most of the time the instruments will not be sampling the same air parcel. Instead there will be some finite distance and time between when the cloud is sampled by the *in situ* instrument and the cloud is sampled by the remote sensing instrument. It is therefore imperative that these spatial and temporal differences be taken into account and ideally minimized when making the comparison. We first address the temporal difference between when the ER-2 and WB-57 sample a region by making a first order correction for the movement of air parcels using the wind velocity measured aboard the WB-57 by the Meteorological Measurement System (MMS). A detailed description of the derivation of wind velocity from MMS measurements is given by *Scott et al.* [1990].

For the cloud encounter shown in Figure 1, the ER-2 took approximately 10 minutes to traverse the cloud and the WB-57 lagged the ER-2 by between 2 and 8 minutes. For each time interval that data are reported along the ER-2 flight track, the air parcels sampled by the WB-57 are advected back to where they would have been at the time the CRS instrument made a measurement. The air parcel sampled by the HV-TW instrument that is nearest to the air parcel sampled by the CRS instrument is then used in the comparison. The result for a cloud sampled during the flight on July 16th is shown in Figure 2, where the black and green points represent the flight tracks of the ER-2 and WB-57, respectively, and the blue triangles correspond to the air parcels sampled by the WB-57 advected by the winds measured along the WB-57 flight track during the time lag between the ER-2

and WB-57 cloud encounter. As is evident in the figure, even within a few minutes there can be considerable movement of air parcels.

Figure 3 shows the *in situ* HV-TW and retrieved CRS IWC plotted versus time along the ER-2 flight track in blue and green, respectively. The left-hand plot shows data taken during a flight transect through a cloud on July 16th between 79600 and 80200 seconds UT. The colored points on the bottom of the plot show the horizontal distance between the air parcels sampled by HV-TW and CRS with dark blue being points separated by a few hundred meters and red being points separated by more than 3 kilometers. The horizontal separation distance is the distance after the air parcels sampled by HV-TW have been advected as described earlier. For the data shown in the left plot of Figure 3, the distance between the air parcels being sampled ranges from a few hundred meters to two kilometers. For this comparison the retrieved IWC agrees with the *in situ* IWC to within 20% and, in general, reproduces the structure of IWC in the cloud.

If we now look at a case where the sampled air parcels are five kilometers away from each other (right plot of Figure 3), the two measurements do not agree because, while the strength and direction of the wind have been accounted for, the IWC in a cloud varies significantly in magnitude and structure even over a few kilometers. This is evident in several other examples where the measurements agree fairly well when the air parcels being sampled are within two kilometers and the comparison breaks down as the distance between the parcels becomes greater than 2 kilometers. This is consistent with the modeled sampling error caused by inadequate spatial overlap discussed in section 4. The maximum acceptable distance for a reasonable comparison will depend on the level of cloud inhomogeneities, with 2 kilometers being the distance associated with the clouds

sampled during CRYSTAL-FACE. By limiting the comparison to flight legs where both the ER-2 and WB-57 were within 2 kilometers of each other, the error caused by insufficient spatial overlap should be small at least for clouds with comparable inhomogeneities. During the month long CRYSTAL-FACE mission there were only 8 flight legs where both aircraft sampled clouds within 2 kilometers of each other. This results in only 37 minutes of data out of approximately 70 hours of flight time.

The comparisons shown in Figure 3 use IWC derived from Z_e using the *Brown and Illingworth* [1995] relationship. However, the parameters in this relationship were derived from tropical cirrus clouds and are possibly not appropriate for the anvil cirrus sampled during CRYSTAL-FACE. In order to determine which IWC-Z_e relationship best fits the CRYSTAL-FACE data, a linear least squares fit to Equation 4 is performed to derive the coefficients a and b for each flight leg where data from HV-TW and CRS are within 2 kilometers. We convert Equation 3 from mm^6m^{-3} because CRS reports Z_e in terms of dB. This results in the linear equation,

$$log_{10}(IWC) = log_{10}(a) + \frac{b}{10} * Z_e \tag{4}$$

The data are fit by minimizing the weighted residuals in both variables. The data are weighted using a 1 dB uncertainty in radar reflectivity and a 15% uncertainty in IWC. Shown in Figure 4 are regressions of $log_{10}(IWC)$ versus Z_e for data that are within 2 kilometers of each other along with the least squares fits to the data. In Figure 4a each of the flight legs is plotted in a different color as indicated by the figure legend. Also shown are the least square fits to each data set. There is considerable variation in the slope of the best fit line between the data sets. However, a single best fit line can be found that fits all the data to within $\pm 20\%$. The least squares fit to all the data is shown

in Figure 4b as a dark-gray thick dashed line. Also shown are the IWC-Z_e relationships using the coefficients from Liu [2000], Brown [1995], and Aydin [1997] as dashed lines in the three lighter shades of gray. The coefficients derived from this work as well as those from previous comparisons are listed in Table 1. The Table also includes characterizations of the clouds used in each study.

Figure 5 shows the eight comparisons that were made during CRYSTAL-FACE. The comparisons are divided by cloud thickness, with thin cirrus plotted in the top four plots and thick cirrus plotted in the bottom four plots. For each comparison plot, the *in situ* IWC data from the HV-TW instrument are plotted in black and the derived IWC data using the fit coefficients from this work are plotted in blue. Also shown are derived IWC data using the relationships described in Brown [1995], Liu [2000], Sassen [1987], and Aydin [1997] in purple, magenta, cyan, and red, respectively. For three of the four thin cirrus cases (Figure 5, plots *a*, *c*, and *d*), the coefficients from this work, as well as those listed in Table 1 agree well with the *in situ* IWC data. In contrast, for the comparison from July 11th (Figure 5, plot *b*), all the relationships underpredict the amount of ice by between 25 and 50%. However, this can possibly be attributed to the predominance of small particles as this is the thinnest cirrus layer presented in this comparison. For the thick cirrus cases, all of which are from July 16th, the agreement between *in situ* and remote data vary between a few percent and 60% depending on which relationship is used. For the comparisons shown in plots *e* and *f*, the Brown [1995], Liu [2000] and coefficients from this work agree with the *in situ* IWC to within 20%. For the comparison shown in plot *g*, the Aydin [1997] and Sassen [1987] give the best agreement, and for the comparison shown in plot *h* none of the parametrizations agree well over the whole flight

leg, with differences ranging from 10 to 30%. However, this is also the case with the worst spatial overlap with distances ranging between 1 and 2.5 km. The comparisons presented in Figures 4 and 5 show that a single IWC-Z_e relationship is able to reproduce the IWC from *in situ* data to within a few percent to 30% depending on the flight leg. The question that now must be addressed is whether this variability in agreement represents variability in the IWC-Z_e relationship or is due to sampling error.

4. Quantifying sampling error due to inadequate spatial overlap

In order to quantify the sampling errors associated with comparing measurements that are not collocated, synthetic clouds, of the type observed during CRYSTAL-FACE, are generated using DHARMA, a cloud resolving microphysics model [*Ackerman et al.*, 2004; *Fridlind et al.*, 2004; *Stevens et al.*, 2002]. The output from the model simulates the cirrus cloud inhomogeneities observed during CRYSTAL-FACE making it well suited for studying the sampling error between measurements that are not collocated. The results presented here use simulations of the clouds sampled by the WB-57 and ER-2 on July 16th and 18th. We use a simulation to evaluate sampling error in order to temporarily remove the uncertainties associated with the instruments or with deriving IWC from Z_e from the analysis. This means that any differences between two synthetic measurements from the simulation must be caused by sampling error resulting from insufficient overlap between the two measurements.

To quantify how close two measurements must be to each other in order to ensure that the sampling error is less than or comparable to the instrument uncertainty we calculate the average error between measurements of IWC by two aircraft flying parallel to each other, but separated by some distance. By using different transects through the simulated

cloud at different altitudes, the sampling error can be calculated for different spatial separations and different levels of cloud inhomogeneity. In Figure 6, IWC is plotted at a particular altitude within a cloud, in this case a simulation of the could system sampled by the WB-57 and ER-2 on July 16th, 2002. The upper contour plot is a horizontal slice through the cloud at an altitude of 16.3 km and the lower contour plot is at an altitude of 15.6 km. Both plots show contours of IWC in g/m^3 as indicated by the color bar to the right of each plot. The graphs below each contour plot show the fractional difference between two measurements separated by a distance of 0 to 10 km for each altitude, with the median value for each separation distance plotted as squares. For the horizontal slice at 16.3 km, the error caused by two aircraft sampling parcels that are separated by 1 km is 15% and by 2 km is 30%. For the horizontal slice at 15.6 km, the error caused by two aircraft sampling parcels that are separated by 1 km is 10% and by 2 km is 20%. It is important to note that the level of inhomogeneities in the cloud have a large vertical dependence, and therefore the restrictions on the coordination of two aircraft may depend both on the type of cloud and location within a particular cloud. To reduce the necessity of coordinating two aircraft to be collocated horizontally to within 1 to 2 km, the *in situ* aircraft would ideally be sampling in the thicker parts of the cirrus.

5. Conclusions

The comparisons between *in situ* IWC and remotely measured Z_e made during the CRYSTAL-FACE mission show a consistent IWC-Z_e relationship for the cirrus clouds sampled over Florida, within the uncertainty due to sampling error. This was the first comparison in which both *in situ* IWC and remote measured Z_e were used, as previous studies relied on converting particle size spectra into IWC and Z_e. The agreement observed

between *in situ* IWC and IWC derived from Z_e is approximately 20% when comparing *in situ* air parcels that were within 2 km of remotely measured air parcels. Previous comparisons based on particle size distributions found errors of +50% to -30% in IWC for a given Z_e [*Liu and Illingworth*, 2000]. Due to the requirement that the air parcels sampled by *in situ* and remote instruments be collocated to within 2 km, during the CRYSTAL-FACE mission only 37 minutes out of more than 70 hours of flight time are usable for direct comparisons. This restriction on which comparisons can be used is important since once the sampling error becomes larger than the instrument uncertainty, it is not possible to distinguish variability in the IWC-Z_e relationship due to microphysical differences between the cloud samples from sampling error. Most of the flight legs presented in this work were made on July 16th, which means that the relationship derived has only been validated for a single cloud. In order to both derive IWC-Z_e relationships for different types of clouds and to validate IWC retrieval algorithms for either airborne- or satellite- based radar, the frequency of valid comparison oppurtunities for a flight mission must be increased.

To quantify the uncertainty associated with sampling error, we have used the DHARMA model to simulate the cirrus sampled during CRYSTAL-FACE. The model predicts that a sampling error of 20 to 30% for air parcels separated by 2 km would be expected for the cirrus encountered during CRYSTAL-FACE. This means that the discrepancies between *in situ* IWC and IWC derived from Z_e during CRYSTAL-FACE are consistent with the expected sampling error due to the measurements not being collocated, and do not indicate that several IWC-Z_e relationships are necessary to explain the clouds sampled during CRYSTAL-FACE. The maximum allowable separation distance will vary for different clouds, since the sampling error depends on cloud inhomogeneities.

While the results from the CRYSTAL-FACE mission seem promising, a much larger data set is needed in order to evaluate how well a single IWC-Z_e relationship describes similar types of clouds. Given the importance of clouds in the climate system and the importance of having quantitative measurements from A-Train satellites, aircraft campaigns will have to be able to provide large quantities of *in situ* data with sufficient overlap in order to quantitatively validate remote sensing instruments.

Acknowledgments. The authors gratefully acknowledge the hard work of the WB-57 and ER-2 pilots and crew during the CRYSTAL-FACE mission. We also thank Dr. Thomas Hanisco for his insightful comments during the preparation of this manuscript. Support from NASA Grants NAG5-11548, NAG5-115487, NAG5-8779, and NAG1-01095 are gratefully acknowledged.

References

Ackerman, A. S., M. P. Kirkpatrick, D. E. Stevens, and O. B. Toon (2004), The impact of humidity above stratiform clouds on indirect aerosol climate forcing, *Nature*, *432*, 1014–1017.

Atlas, D., S. Y. Matrosov, A. J. Heymsfield, M.-D. Chou, and D. B. Wolf (1995), Radar and radiation properties of ice clouds, *Journal of Applied Meteorology*, *34*, 2329–2345.

Aydin, K., and C. X. Tang (1997), Relationships between iwc and polarimetric radar measurands at 94 and 220 ghz for hexagonal columns and plates, *Journal Of Atmospheric And Oceanic Technology*, *14*, 1055–1063.

Baran, A. J. (2005), The dependence of cirrus infrared radiative properties on ice crystal geometry and shape of the size-distribution function, *Quarterly Journal of the Royal*

375 *Meteorological Society, 131*(607), 1129–1142.

376 Brown, P. R. A., and A. J. Illingworth (1995), The role of spaceborne millimeter-wave
377 radar in the global monitoring of ice cloud, *Journal of Applied Meteorology, 34*, 2346–
378 2366.

379 Buschmann, N., G. M. McFarquhar, and A. J. Heymsfield (2002), Effects of observed
380 horizontal inhomogeneities within cirrus clouds on solar radiative transfer, *Journal Of*
381 *Geophysical Research-Atmospheres, 107.*

382 Donovan, D. P. (2003), Ice-cloud effective particle size parameterization based on com-
383 bined lidar, radar reflectivity, and mean doppler velocity measurements, *Journal Of*
384 *Geophysical Research-Atmospheres, 108.*

385 Fridlind, A. M., A. S. Ackerman, E. J. Jensen, A. J. Heymsfield, M. R. Poellot, D. E.
386 Stevens, D. Wang, L. M. Miloshevich, D. Baumgardner, R. P. Lawson, J. C. Wilson,
387 R. C. Flagan, J. H. Seinfeld, H. H. Jonsson, T. M. VanReken, V. Varutbangkul, and
388 T. A. Rissman (2004), Evidence for the predominance of mid-tropospheric aerosols as
389 subtropical anvil nuclei, *Science, 304*, 718–722.

390 Gultepe, I., G. A. Isaac, and K. B. Strawbridge (2001), Variability of cloud microphysical
391 and optical parameters obtained from aircraft and satellite remote sensing measure-
392 ments during race, *International Journal Of Climatology, 21*, 507–+.

393 Jensen, E., D. Starr, and O. B. Toon (2004), Mission investigates tropical cirrus clouds,
394 *Eos Trans. AGU, 84*(5), 50.

395 Li, L. H., G. M. Heymsfield, P. E. Racette, L. Tian, and E. Zenker (2004), A 94-ghz
396 cloud radar system on a nasa high-altitude er-2 aircraft, *Journal Of Atmospheric And*
397 *Oceanic Technology, 21*, 1378–1388.

Liao, L., and K. Sassen (1994), Investigation of relationships between Ka-band radar reflectivity and ice and liquid water contents, *Atmospheric Research*, *34*, 231–248.

Liu, C. L., and A. J. Illingworth (2000), Toward more accurate retrievals of ice water content from radar measurements of clouds, *Journal Of Applied Meteorology*, *39*, 1130–1146.

Nasiri, S. L., B. A. Baum, A. J. Heymsfield, P. Yang, M. R. Poellot, D. P. Kratz, and Y. X. Hu (2002), The development of midlatitude cirrus models for modis using fire-i, fire-ii, and arm in situ data, *Journal Of Applied Meteorology*, *41*, 197–217.

Norris, J. R. (2000), What can cloud observations tell us about climate variability?, *Space Science Reviews*, *94*, 375–380.

Pawlowska, H., J. L. Brenguier, Y. Fouquart, W. Armbruster, S. Bakan, J. Descloitres, J. Fischer, C. Flamant, A. Fouilloux, J. F. Gayet, S. Gosh, P. Jonas, F. Parol, J. Pelon, and L. Schuller (2000), Microphysical and radiative properties of stratocumulus clouds: the eucrex mission 206 case study, *Atmospheric Research*, *55*, 85–102.

Sassen, K., Z. Wang, V. I. Khvorostyanov, G. L. Stephens, and A. Bennedetti (2002), Cirrus cloud ice water content radar algorithm evaluation using an explicit cloud microphysical model, *Journal Of Applied Meteorology*, *41*, 620–628.

Scott, S. G., T. P. Bui, K. R. Chan, and S. W. Bowen (1990), The meteorological measurement system on the NASA ER-2 aircraft, *Journal of Atmospheric and Oceanic Technology*, *7*(4), 525–540.

Stephens, G. L. (2005), Cloud feedbacks in the climate system: a critical review, *Journal of Climate*, *18*, 237–273.

Stephens, G. L., D. G. Vane, R. J. Boain, G. G. Mace, K. Sassen, Z. E. Wang, A. J. Illingworth, E. J. O'Connor, W. B. Rossow, S. L. Durden, S. D. Miller, R. T. Austin, A. Benedetti, and C. Mitrescu (2002), The cloudsat mission and the a-train - a new dimension of space-based observations of clouds and precipitation, *Bulletin Of The American Meteorological Society*, *83*, 1771–1790.

Stevens, D. E., A. S. Ackerman, and C. S. Bretherton (2002), Effect of domain size and numerical resolution on the simulation of shallow cumulus convection, *Journal Of Atmospheric Science*, *59*, 3285–3301.

Wang, Z., and K. Sassen (2002a), Cirrus cloud microphysical property retrieval using lidar and radar measurements. part i: Algorithm description and comparison with in situ data, *Journal Of Applied Meteorology*, *41*, 218–229.

Wang, Z., and K. Sassen (2002b), Cirrus cloud microphysical property retrieval using lidar and radar measurements. part ii: Midlatitude cirrus microphysical and radiative properties, *Journal Of The Atmospheric Sciences*, *59*, 2291–2302.

Weinstock, E. M., J. B. Smith, D. Sayres, J. V. Pittman, N. Allen, and J. G. Anderson (2006a), Measurements of the total water content of cirrus clouds. part ii: Instrument performance and validation, *JOURNAL OF ATMOSPHERIC AND OCEANIC TECHNOLOGY*, *23*(11), 1410–1421.

Weinstock, E. M., J. B. Smith, D. Sayres, J. R. Spackman, J. V. Pittman, N. Allen, J. Demusz, M. Greenberg, M. Rivero, L. Solomon, and J. G. Anderson (2006b), Measurements of the total water content of cirrus clouds. part i: Instrument details and calibration, *JOURNAL OF ATMOSPHERIC AND OCEANIC TECHNOLOGY*, *23*(11), 1397–1409.

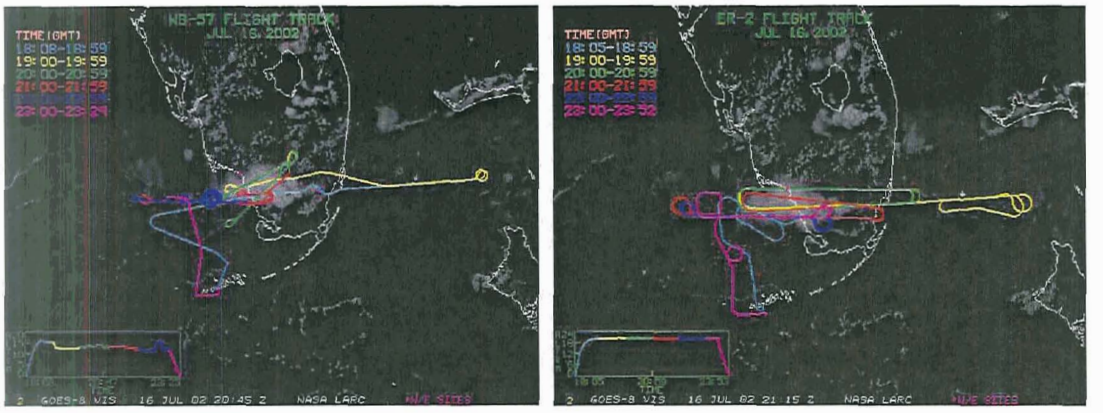

Figure 1. The image on the left shows the flight track of the WB-57 on July 16, 2002 superimposed over a visible GOES image taken at 20:45 UT on July 16th. The flight track is divided into six color coded legs as described by the legend in the image. The image on the right shows the flight track of the ER-2 on July 16, 2002 superimposed over a visible GOES image taken at 21:15 UT on July 16. The legs are divided into approximately the same times periods as with the WB-57. Also shown are the altitudes the aircraft flew at in the lower left hand corner of each image.

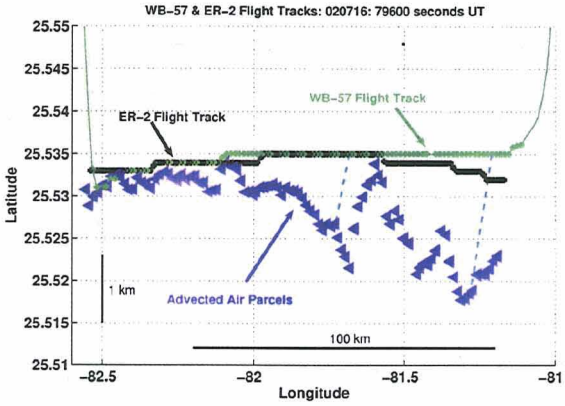

Figure 2. Advection of air parcels between when the ER-2 and WB-57 sampled the same region. The black points represent the ER-2 flight track, the green points represent the WB-57 flight track and the blue triangles correspond to the air parcels sampled by the WB-57 advected back to where they would have been when the ER-2 sampled this region. The light blue dashed lines show the advection of selected air parcels during the time lag between the ER-2 and WB-57. Note that the x- and y-axes have different scales as indicated by the black scale lines in the figure.

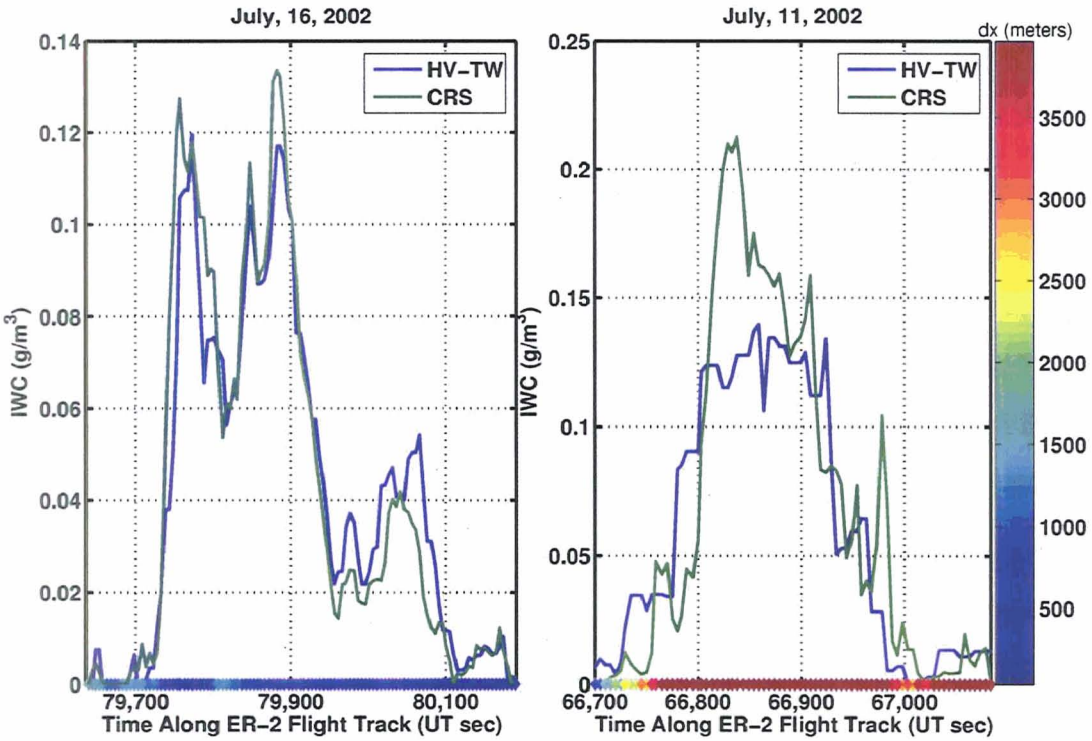

Figure 3. Comparison of IWC measured *in situ* by the Harvard Total Water instrument and derived from the remote Cloud Radar System, during a cloud transect on July 16th at 79600 seconds UT (left plot) and July 11th at 66700 seconds UT (right plot). HV-TW is plotted in blue and CRS is plotted in green versus time along the ER-2 flight track. The colored points along the bottom of the plots represent the horizontal distance between the air parcels sampled by both instruments. The color code is given by the vertical colorbar to the right of the figures.

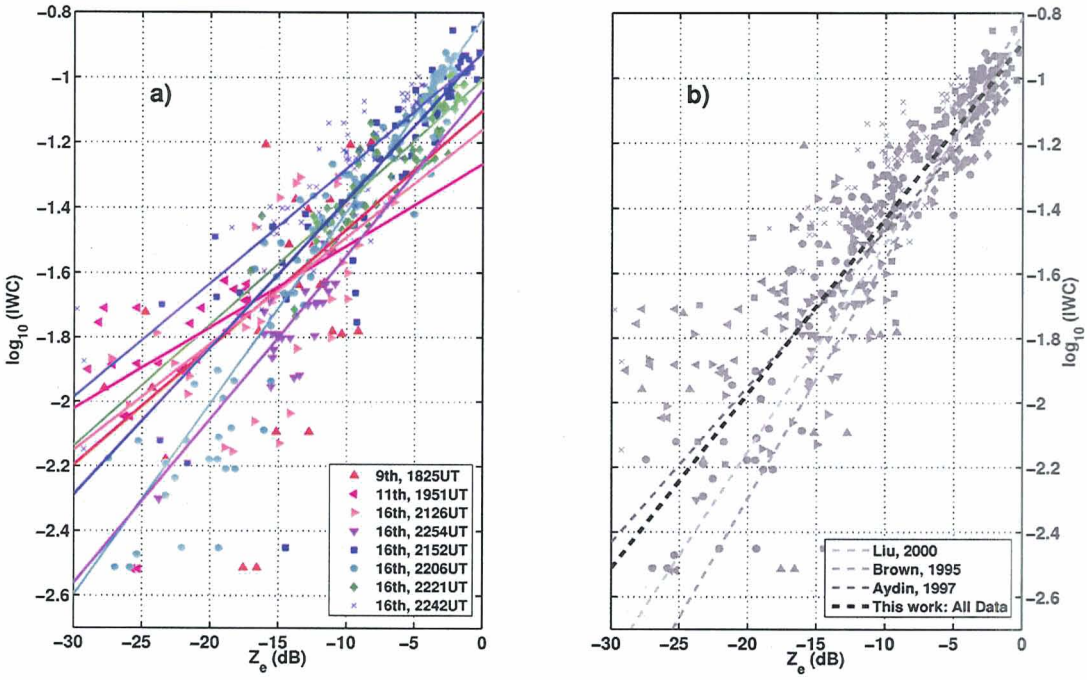

Figure 4. Scatter plots of Z_e (dB) from CRS versus $log_{10}(IWC)$ from HV-TW for 8 different flight segments. Plot a) Each flight segment is plotted in a different color according to the legend in the figure. Colored lines are linear least square fits to the data from each flight segment. Plot b) Plot of all data from the 8 flight segments as well as the least square fit to all the data shown as a thick dark gray dashed line. Also shown are fits using coefficients from Liu [2000], Brown [1995] and Aydin [1997] in the lighter shades of gray.

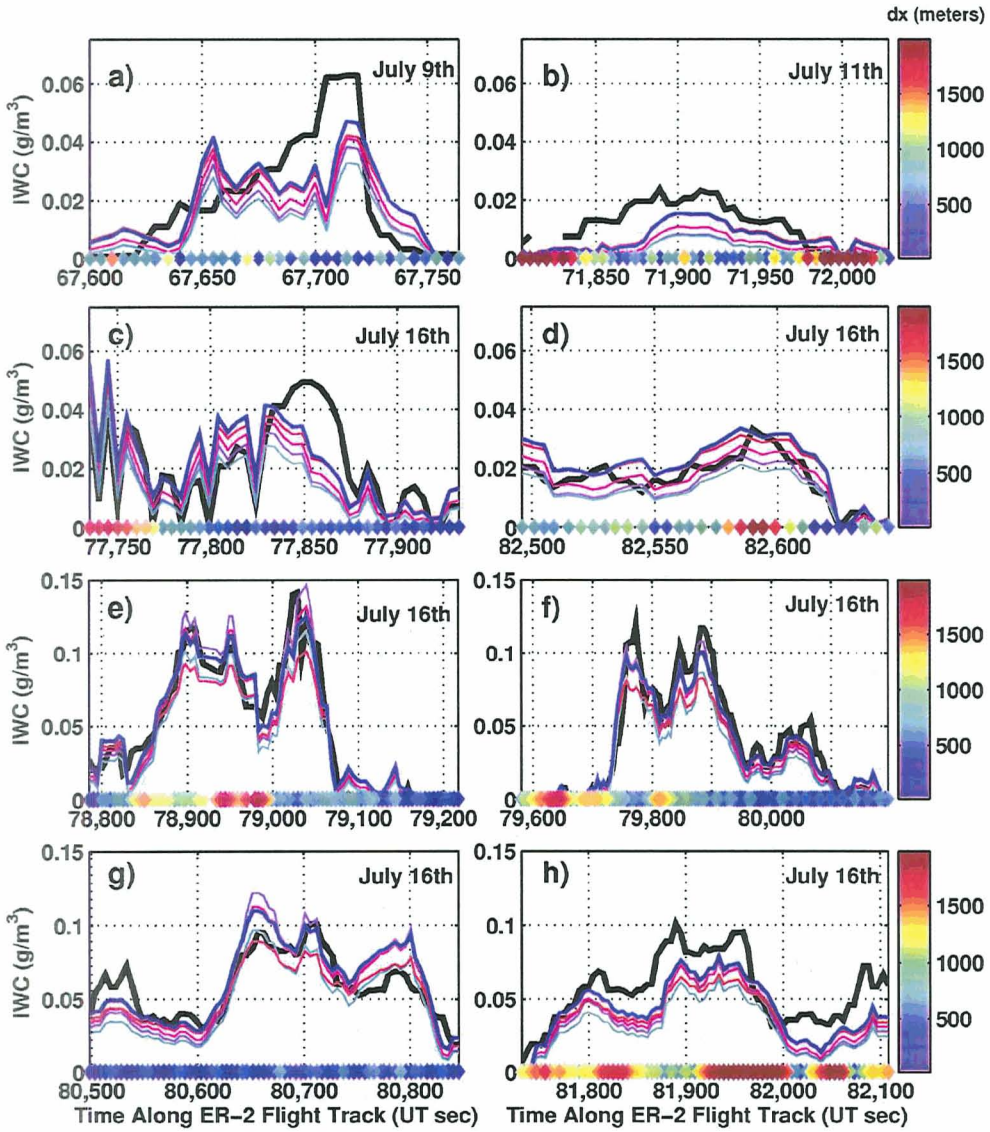

Figure 5. The 8 plots represent all the comparisons that were made during CRYSTAL-FACE where the air parcels sampled by the WB-57 and ER-2 were within 2 km of each other. For each comparison, the *in situ* IWC data are plotted in black and the derived IWC data using parameters obtained from this work are plotted blue. Also shown are derived IWC data using the relationships described in Brown [1995], Liu [2000], Sassen [1987], and Aydin [1997] in purple, magenta, cyan, and red, respectively.

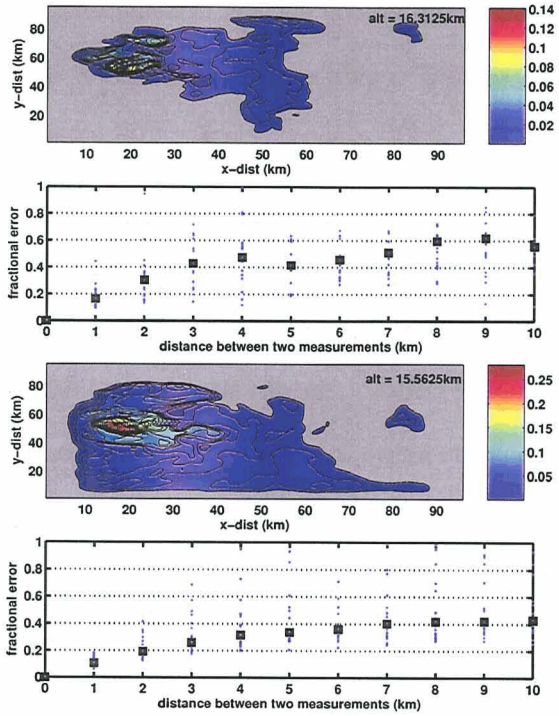

Figure 6. Contour plots show IWC (g/m^3) from the cloud model at altitudes of 16.3 and 15.6 km. The bottom graphs show the fractional error between two measurements of the same cloud as the distance between the measurements increases from 0 to 10 km. The blue points are the average fractional error calculated between two random trajectories through the cloud separated by a distance of 0 to 10 km. The black squares are the median values at each distance for 10 random trajectories.

Table 1. Parameters for IWC-Z_e relationships from several sources. Coefficients a and b are least squares fits to $IWC = aZ_e^b$ where IWC is measured in g/m^3 and Z_e is measured in mm^6m^{-3}.

Source	Cloud Type	Source of IWC/Z_e	a	b
Sassen, 1987	ground measurements, precipitating ice crystals	size spectra / radar	0.12	0.696
Brown, 1995	N. latitude frontal systems & tropical cirrus	in situ size spectra	0.153	0.74
Liu, 2000	N. latitude frontal systems & tropical cirrus	in situ size spectra	0.137	0.643
Atlas, 1995	midlatitude clouds	in situ size spectra	0.064	0.58
Aydin, 1997	hexagonal columns and plates	modeled size spectra	0.104	0.483
This work	midlatitude anvil cirrus	in situ / radar	0.13	0.54